ACS Medicinal Chemistry Letters

Letter

pubs.acs.org/acsmedchemlett

Structure–Activity Relationships and in Vivo Evaluation of Quinoxaline Derivatives for PET Imaging of β-Amyloid Plaques

Masashi Yoshimura,[†] Masahiro Ono,*[,†] Kenji Matsumura,[†] Hiroyuki Watanabe,[†] Hiroyuki Kimura,[†] Mengchao Cui,[†] Yuji Nakamoto,[‡] Kaori Togashi,[‡] Yoko Okamoto,[§] Masafumi Ihara,[§] Ryosuke Takahashi,[§] and Hideo Saji[†]

[†]Department of Patho-Functional Bioanalysis, Graduate School of Pharmaceutical Sciences, Kyoto University, 46-29 Yoshida Shimoadachi-cho, Sakyo-ku, Kyoto 606-8501, Japan

[‡]Department of Diagnostic Imaging and Nuclear Medicine, Graduate School of Medicine, Kyoto University, 54 Shogoin Kawahara-cho, Sakyo-ku, Kyoto 606-8507, Japan

[§]Department of Neuroscience, Graduate School of Medicine, Kyoto University, 54 Shogoin Kawahara-cho, Sakyo-ku, Kyoto 606-8507, Japan

Supporting Information

ABSTRACT: This letter describes the synthesis, structure–activity relationships, and in vivo evaluation of a new series of 2-phenylquinoxaline (PQ) derivatives for imaging β-amyloid (Aβ) plaques in Alzheimer's disease (AD). In experiments in vitro, the affinity of the derivatives for Aβ aggregates varied, with K_i values of 0.895 to 1180 nM. In brain sections from AD patients, derivatives with a K_i of less than 111 nM intensely labeled Aβ plaques, while those with values over 242 nM showed no marked labeling. In biodistribution experiments using normal mice, the derivatives showed good uptake into (4.69–7.59 %ID/g at 2 or 10 min postinjection) and subsequent washout from (1.48–3.08 %ID/g at 60 min postinjection) the brain. In addition, [^{18}F]PQ-6 labeled Aβ plaques in vivo in APP transgenic mice, while it showed nonspecific binding in the white matter. Further structural optimization based on [^{18}F]PQ-6 may lead to more useful PET probes for imaging Aβ plaques.

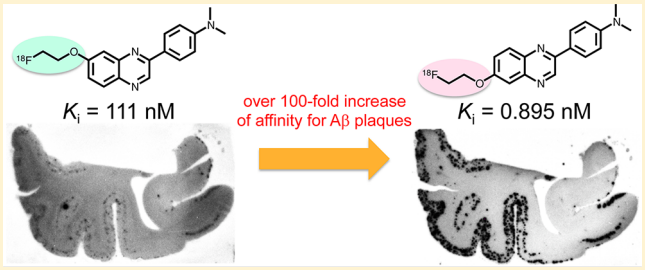

KEYWORDS: *Alzheimer's disease (AD), β-amyloid (Aβ), PET, quinoxaline, structure–activity relationships*

Alzheimer's disease (AD) is a leading cause of dementia with symptoms including progressive memory loss and an inability to carry out normal daily functions. As populations continue to age rapidly all over the world, the increase in the number of AD patients constitutes a serious social issue. However, no diagnostic or therapeutic methods have been established for AD.[1] Post-mortem brains of AD patients reveal senile plaques (SPs) composed of β-amyloid (Aβ) peptides and neurofibrillary tangles (NFTs) formed by hyperphosphorylated tau proteins.[2] Although the precise molecular mechanisms causing AD remain unknown, the amyloid cascade hypothesis, that SPs play an important role in its development, is widely accepted.[3,4] Consequently, the in vivo imaging of SPs composed of Aβ plaques with noninvasive techniques such as positron emission tomography (PET) or single photon emission computed tomography (SPECT) could be useful for the presymptomatic diagnosis of AD and new antiamyloid therapies.

Toward this end, great efforts have been made to develop PET and SPECT probes that can image Aβ plaques in vivo. Several PET probes have undergone clinical studies. [^{11}C]PIB ([^{11}C]-2-(4′-methylaminophenyl)-6-hydroxybenzothiazole), a neutral thioflavin T (ThT) analogue, has been widely used in AD research because one can clearly distinguish between AD patients and healthy controls from the high signal-to-noise ratio.[5−7] More recently, a stilbene analogue with fluorinated polyethylene glycol (PEG) units, [^{18}F]-(*E*)-4-(2-(6-(2-(2-(2-fluoroethoxy)ethoxy)ethoxy)pyridin-3-yl)vinyl)-*N*-methylaniline ([^{18}F]AV-45, Florbetapir), has been approved by the US Food and Drug Administration (FDA) for clinical AD diagnosis by exclusion.[8−10] Other ^{18}F-labeled probes including [^{18}F]-(*E*)-4-(*N*-methylamino)-4′-(2-(2-(2-fluoroethoxy)ethoxy)ethoxy)-stilbene ([^{18}F]BAY94−9172, Florbetaben)[11−13] and 2-(3-[^{18}F]fluoro-4-methylaminophenyl)benzothiazol-6-ol ([^{18}F]GE-067, Flutemetamol)[14,15] are expected to obtain FDA approval in the near future.

Recently, we have developed a new type of probe based on the quinoxaline pharmacophore.[16,17] These derivatives displayed high affinity for Aβ aggregates with K_i values in the nM range (4.1−10.7 nM) and showed specific labeling of Aβ plaques in sections of brain tissue from AD patients and transgenic mice. In biodistribution experiments, these probes

Received: February 19, 2013
Accepted: May 8, 2013
Published: May 21, 2013

showed high initial uptake into the brain (2.49−8.17 %ID/g at 2 min) and subsequently washed out from the brain with time. These previous results suggested that quinoxaline may serve as a new scaffold for the development of more useful PET probes. In the present study, to further examine structure−activity relationships on affinity for Aβ aggregates and pharmacokinetics in vivo, we designed and synthesized new fluorinated PQ derivatives which have a fluoropegylated group at position 6 or 7 of the PQ structure.

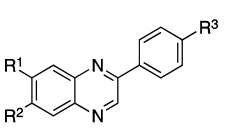

[^{18}F]PQ-1 (R^1 = $OCH_2CH_2{}^{18}F$, R^2 = H, R^3 = NH_2)
[^{18}F]PQ-2 (R^1 = $OCH_2CH_2{}^{18}F$, R^2 = H, R^3 = $NHCH_3$)
[^{18}F]PQ-3 (R^1 = $OCH_2CH_2{}^{18}F$, R^2 = H, R^3 = $N(CH_3)_2$)
[^{18}F]PQ-4 (R^1 = H, R^2 = $OCH_2CH_2{}^{18}F$, R^3 = NH_2)
[^{18}F]PQ-5 (R^1 = H, R^2 = $OCH_2CH_2{}^{18}F$, R^3 = $NHCH_3$)
[^{18}F]PQ-6 (R^1 = H, R^2 = $OCH_2CH_2{}^{18}F$, R^3 = $N(CH_3)_2$)

Figure 1. Chemical structure of fluoropegylated PQ derivatives.

The synthesis of 7-fluoropegylated and 6-fluoropegylated PQ derivatives is outlined in Schemes 1 and 2, respectively. The details of the synthesis are described in the Supporting Information.

The desired ^{18}F-labeled PQ derivatives were prepared via a nucleophilic displacement reaction with a fluoride anion as shown in Scheme 3. To prepare the desired ^{18}F-labeled dimethylated PQ derivatives, the tosylate precursors (**16** and **34**) were reacted with [^{18}F]fluoride/potassium carbonate and Kryptofix 222 in acetonitrile. Radiolabeling with ^{18}F was successfully performed on the precursor to generate [^{18}F]PQ-3 and [^{18}F]PQ-6 with radiochemical yields of 31.3 ± 16.0% (n = 8) and 19.6 ± 11.4% (n = 5), respectively. To prepare the desired ^{18}F-labeled nonmethylated and monomethylated PQ derivatives, the *N*-Boc-protected tosylates **21**, **22**, **35**, and **36** were employed as the precursors. Each of the tosylates was reacted with [^{18}F]fluoride/potassium carbonate and Kryptofix 222 in acetonitrile. The mixture was then treated with aqueous HCl to remove the *N*-Boc-protected group. Radiolabeling with ^{18}F was successfully performed on the precursor to generate [^{18}F]PQ-1, [^{18}F]PQ-2, [^{18}F]PQ-4, and [^{18}F]PQ-5 with radiochemical yields of 25.9 ± 12.5% (n = 3), 20.1 ± 8.9% (n = 3), 34.0 ± 9.5% (n = 3), and 22.7 ± 5.5% (n = 3), respectively. Each radiolabeling was accomplished with a radiochemical purity greater than 95%. The identity of radioactive PQ derivatives was verified by a comparison of the retention time with that of the nonradioactive compound.

In vitro binding experiments to evaluate the affinity of the 6 PQ derivatives for Aβ_{1-42} aggregates were carried out in solutions with [^{125}I]6-iodo-2-(4′-*N*,*N*-dimethylamino)-phenylimidazo[1,2-a]pyridine ([^{125}I]IMPY) as the competing ligand. AV-45 was also tested using the same system for comparison. The results are listed in Table 1. The affinity of PQ derivatives for Aβ aggregates varied, with K_i values of 0.895 to 1180 nM. The 6-fluoropegylated as well as 7-fluoropegylated PQ derivatives had affinity for Aβ aggregates in the following order: dimethylamino derivatives > monomethylamino derivatives > primary amino derivatives. The results of the binding experiments were consistent with those of some previous studies.[18−20] Furthermore, the affinity of 6-fluoropegylated PQ derivatives (K_i = 0.895−242 nM) was much higher than that of the corresponding 7-fluoropegylated PQ derivatives (K_i = 111−1180 nM), indicating that the substituted site of the fluoropegylated group in the PQ scaffold plays an important role in the binding to Aβ aggregates. Among the 6 PQ

Scheme 1[a]

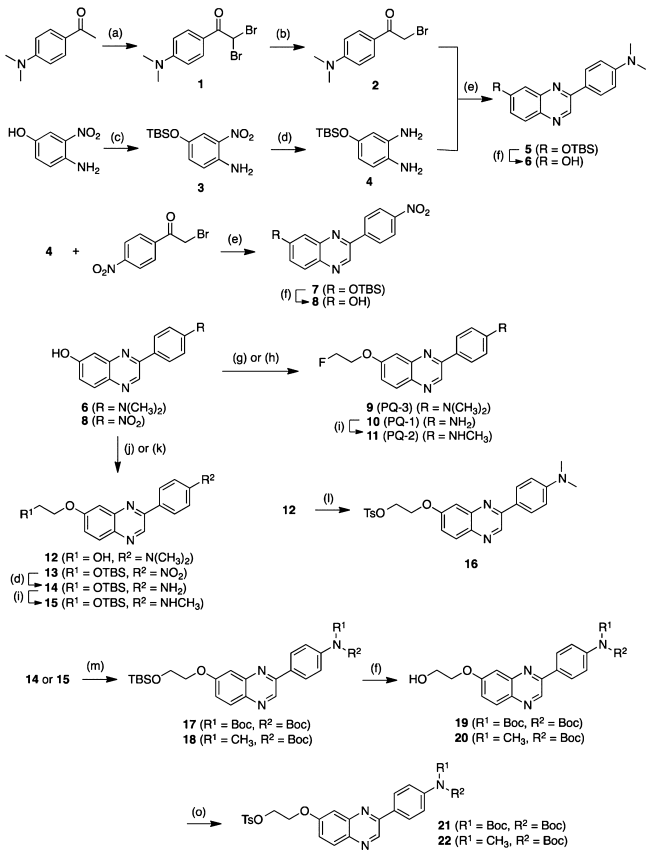

[a]Reagents and conditions: (a) Br_2, H_2SO_4, 0 °C to rt; (b) diethyl phosphite, triethylamine, THF, 0 °C to rt; (c) TBSCl, imidazole, THF, rt; (d) H_2, Pd/C, MeOH, CH_2Cl_2, rt; (e) DMSO, rt; (f) TBAF, THF, 0 °C to rt; (g) 2-fluoroethyl 4-methylbenzenesulfonate, K_2CO_3, DMF, 105 °C; (h) (1) 2-fluoroethyl 4-methylbenzenesulfonate, K_2CO_3, DMF, 105 °C, (2) H_2, Pd/C, MeOH, CH_2Cl_2, rt; (i) (1) paraformaldehyde, NaOMe, MeOH, 0 °C to reflux, (2) $NaBH_4$, reflux; (j) 2-bromoethanol, K_2CO_3, DMF, 105 °C; (k) (2-bromoethoxy)-*tert*-butyldimethylsilane, K_2CO_3, DMF, 80 °C; (l) TsCl, pyridine, 0 °C to rt; (m) Boc_2O, DMAP, triethylamine, THF, reflux; (o) TsCl, DMAP, pyridine, 0 °C to rt.

derivatives, PQ-6 showed the highest affinity for Aβ aggregates with a K_i of 0.895 nM. The binding of [^{18}F]PQ-6 with the fluoroethyleneoxy group at position 6 in the PQ scaffold was over 100-fold that of [^{18}F]PQ-3 with the fluoroethyleneoxy group at position 7. Furthermore, in comparison with AV-45, the only such compound approved by the FDA, the affinity of PQ-6 increased about 10-fold, suggesting the potential utility of [^{18}F]PQ-6 for imaging Aβ plaques in AD brain.

The binding of six [^{18}F]PQ-1−6 derivatives or [^{18}F]AV-45 as a positive control to Aβ plaques in brain sections from AD patients was evaluated by autoradiography in vitro. As shown in Figure 2, [^{18}F]PQ-5 and [^{18}F]PQ-6 with a K_i of 15.7 and 0.895 nM, respectively, intensively labeled Aβ plaques showing a strong signal in the cortex region and a low background level in the white matter. [^{18}F]PQ-3 with a K_i of 111 nM showed moderate binding and labeled only a few Aβ plaques. Conversely, [^{18}F]PQ-1, [^{18}F]PQ-2, and [^{18}F]PQ-4 with K_i values above 242 nM did not display marked binding to Aβ plaques although they showed high nonspecific binding in the white matter region. The results of autoradiography in vitro were consistent with those of binding assays in vitro, and also

dx.doi.org/10.1021/ml4000707 | ACS Med. Chem. Lett. 2013, 4, 596−600

Scheme 2[a]

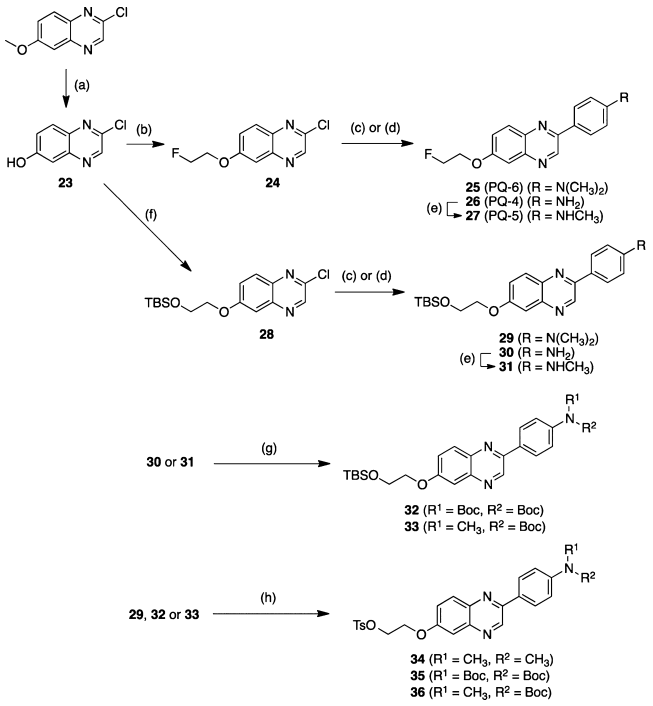

[a]Reagents and conditions: (a) $AlCl_3$, toluene, 0 to 80 °C; (b) 2-fluoroethyl 4-methylbenzenesulfonate, K_2CO_3, DMF, 80 °C; (c) *N*,*N*-dimethyl-4-(4,4,5,5-tetramethyl-1,3,2-dioxaborolan-2-yl)aniline, $Pd(PPh_3)_4$, K_2CO_3 aq. (2 M), toluene, EtOH, reflux; (d) 4-(4,4,5,5-tetramethyl-1,3,2-dioxaborolan-2-yl)aniline, $Pd(PPh_3)_4$, K_2CO_3 aq. (2 M), toluene, EtOH, reflux; (e) (1) paraformaldehyde, NaOMe, MeOH, 0 °C to reflux, (2) $NaBH_4$, reflux; (f) (2-bromoethoxy)-*tert*-butyldimethylsilane, K_2CO_3, DMF, 80 °C; (g) Boc_2O, DMAP, triethylamine, THF, reflux; (h) (1) TBAF, THF, 0 °C to rt, (2) TsCl, DMAP, pyridine, rt.

Scheme 3[a]

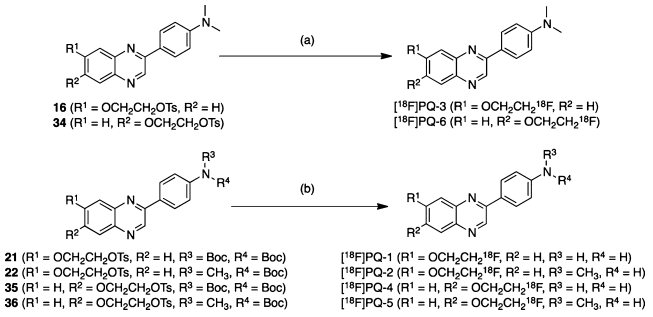

[a]Reagents and conditions: (a) $^{18}F^-$, K_2CO_3, Kryptofix222, acetonitrile, 100 °C; (b) (1) $^{18}F^-$, K_2CO_3, Kryptofix222, acetonitrile, 100 °C, (2) HCl (1 M), 100 °C.

suggested that the substituted site of the fluoroethylene group in the PQ moiety may strongly affect the affinity of the PQ derivatives for Aβ aggregates.

Next, all of the ^{18}F-labeled PQ derivatives were evaluated for their biodistribution in normal mice. We carried out the biodistribution study using [^{18}F]AV-45 as a control under similar experimental conditions. To compare the uptake into and washout from the brain, a combined plot is presented in Figure 3. All PQ derivatives displayed a high uptake, 4.69−7.59 %ID/g, at 2 or 10 min postinjection, indicating that they,

Table 1. Inhibition Constants (K_i, nM) for the Binding of [^{125}I]IMPY to Aβ_{1-42} Aggregates

compd	K_i (nM)[a]
PQ-1	1180 ± 370
PQ-2	758 ± 83.8
PQ-3	111 ± 13.2
PQ-4	242 ± 29.0
PQ-5	15.7 ± 1.28
PQ-6	0.895 ± 0.141
AV-45	12.8 ± 2.10
IMPY	7.21 ± 1.23

[a]Values are the means ± standard errors of the mean of 6−13 independent determinations.

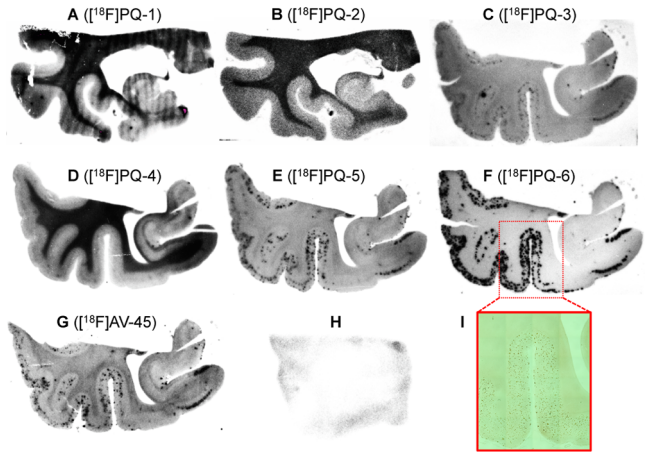

Figure 2. In vitro autoradiogram of AD brain sections (A−G) labeled with [^{18}F]PQ-1−6 and [^{18}F]AV-45, respectively. In vitro autoradiogram of [^{18}F]PQ-6 in a brain section from a healthy control (H). The Aβ plaques were confirmed by immunostaining with an anti-Aβ_{1-42} antibody (I).

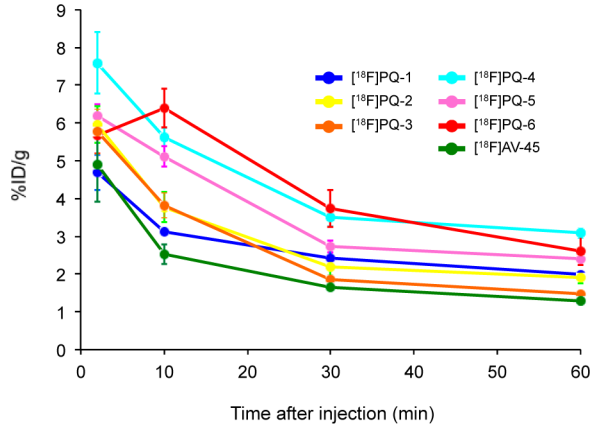

Figure 3. Comparison of brain uptake of [^{18}F]PQ-1−6 and [^{18}F]AV-45 in normal mice.

except [^{18}F]PQ-1, show a higher initial brain uptake than [^{18}F]AV-45. Subsequently, the radioactivity in the brain cleared with time (1.48−3.08 %ID/g at 60 min postinjection). Since there are no Aβ plaques in normal mice, a high initial uptake and rapid washout in normal brain are highly desirable properties for the imaging of Aβ plaques in vivo. When we caluculated the $brain_{2min}/brain_{60min}$ ratio (see Supporting Information, Table S8) to compare the washout rate,

dx.doi.org/10.1021/ml4000707 | ACS Med. Chem. Lett. 2013, 4, 596−600

[^{18}F]PQ-3 (3.91) showed faster clearance than [^{18}F]AV-45 (3.80). Conversely, a slightly slower clearance than [^{18}F]AV-45 was observed for the other derivatives (2.36−3.12). Considering the results of the binding to Aβ plaques in vitro together with the biodistribution studies in vivo, we selected [^{18}F]PQ-6 for further characterization in living brain tissue.

We carried out autoradiography ex vivo with [^{18}F]PQ-6 in Tg2576 and wild-type mice. Tg2576 mice show marked Aβ deposition in the brain by 11−13 months of age and have been frequently used to evaluate the specific binding of Aβ plaques in experiments in vitro and in vivo.[21−24] Ex vivo autoradiograms after the injection of [^{18}F]PQ-6 into a Tg2576 mouse showed extensive labeling of Aβ plaques in the brain (Figure 4A). No

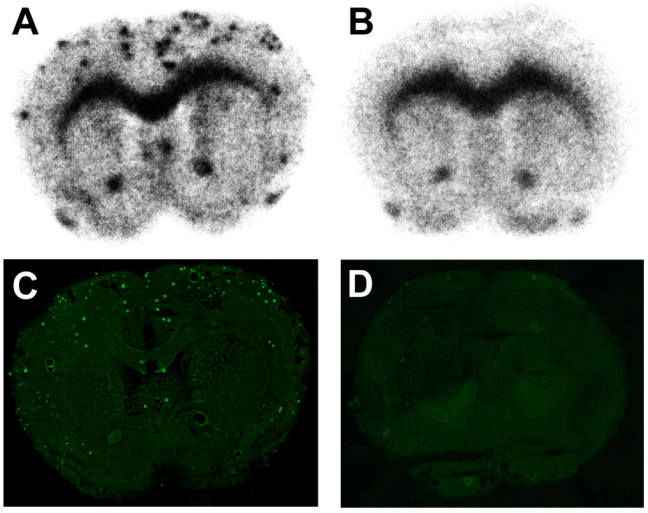

Figure 4. Ex vivo autoradiogram from a Tg2576 mouse (A) and a wild-type mouse (B) with [^{18}F]PQ-6. The same sections (A,B) were also stained with thioflavin-S (C and D, respectively).

such labeling was observed in the wild-type mouse brain (Figure 4B). However, both brains showed high nonspecific radioactivity accumulation despite that [^{18}F]PQ-6 displayed not only washout with time from the normal mouse brain in biodistribution studies but also low nonspecific radioactivity accumulation in white matter in the AD brain in vitro. This high nonspecific radioactivity accumulation was observed in the corpus callosum, external capsule, anterior commissure, and olfactory tract in the mouse brain. These areas are known to have a high density of myelin sheaths, suggesting that [^{18}F]PQ-6 may bind to myelin fibers in the white matter. We also carried out autoradiography ex vivo in Tg2576 and wild-type mice with [^{18}F]PQ-3. Different from [^{18}F]PQ-6, [^{18}F]PQ-3 exhibited no marked specific binding to Aβ plaques in the autoradiograms (see Supporting Information, Figure S1). These results reflected the finding that the affinity of PQ-3 in the binding assay was over 100-fold lower than that of PQ-6, in addition to the marked difference in the autoradiographic experiments using AD brain sections.

In conclusion, we designed and synthesized new 6 PQ derivatives and evaluated their structure−activity relationship to Aβ aggregates and their biodistribution in normal mice. In binding assays, PQ-6 showed the highest affinity for Aβ aggregates with a K_i of 0.895 nM. The affinity of PQ derivatives to Aβ aggregates significantly differed with the substituted position of the fluoroethoxy group in the PQ scaffold. As reflected by the extremely high binding affinity, [^{18}F]PQ-6 also showed the clearest labeling of Aβ plaques in the brain sections from AD patients. In biodistribution studies, PQ derivatives displayed good uptake into and washout with time from the brain. Their radioactivity profiles in the brain were comparable to that of [^{18}F]AV-45. In addition, ex vivo autoradiograms of brain sections from Tg2576 mice after the injection of [^{18}F]PQ-6 showed the feasibility of imaging Aβ plaques, although nonspecific binding was also observed. Further structural optimization based on [^{18}F]PQ-6 to reduce nonspecific binding in the white matter may lead to more useful PET probes for imaging Aβ plaques in the brain.

■ ASSOCIATED CONTENT

Supporting Information

Results of the partition coefficient values, the biodistribution experiments for all organs, and the autoradiography ex vivo using a Tg2576 mouse with [^{18}F]PQ-3, procedures for the preparation of PQ-1−6 and [^{18}F]PQ-1−6, partition coefficient, binding assays using Aβ_{1-42} aggregates, autoradiography in vitro using brain tissue from AD patients, biodistribution in vivo in normal mice, and autoradiography ex vivo using Tg2576 mice. This material is available free of charge via the Internet at http://pubs.acs.org.

■ AUTHOR INFORMATION

Corresponding Author

*(M.O.) Phone: +81-75-753-4608. Fax: +81-75-753-4568. E-mail: ono@pharm.kyoto-u.ac.jp.

Funding

This research was granted by the Japan Society for the Promotion of Science (JSPS) through the "Funding Program for Next Generation World-Leading Researchers (NEXT Program)," initiated by the Council for Science and Technology Policy (CSTP).

Notes

The authors declare no competing financial interest.

■ ABBREVIATIONS

Aβ, β-amyloid; AD, Alzheimer's disease; SP, senile plaque; NFT, neurofibrillary tangle; PET, positron emission tomography; SPECT, single photon emission computed tomography; ThT, thioflavin T; TBSCl, *tert*-butyldimethylsilyl chloride; TBAF, tetrabutylammonium fluoride; NaOMe, sodium methoxide; THF, tetrahydrofuran; Boc, *tert*-butoxycarbonyl; TsCl, *p*-toluenesulfonyl chloride; DMAP, *N*,*N*-dimethyl-4-aminopyridine; IMPY, 6-iodo-2-(4′-*N*,*N*-dimethylamino)phenylimidazo-[1,2-a]pyridine

■ REFERENCES

(1) Holtzman, D. M.; Morris, J. C.; Goate, A. M. Alzheimer's disease: the challenge of the second century. *Sci. Transl. Med.* **2011**, *3*, 77sr1.

(2) Selkoe, D. J. Alzheimer's disease: genes, proteins, and therapy. *Physiol. Rev.* **2001**, *81*, 741−766.

(3) Hardy, J.; Selkoe, D. J. The amyloid hypothesis of Alzheimer's disease: progress and problems on the road to therapeutics. *Science* **2002**, *297*, 353−356.

(4) Finder, V. H. Alzheimer's disease: a general introduction and pathomechanism. *J. Alzheimer's Dis.* **2010**, *22* (Suppl. 3), S5−S19.

(5) Klunk, W. E.; Engler, H.; Nordberg, A.; Wang, Y.; Blomqvist, G.; Holt, D. P.; Bergstrom, M.; Savitcheva, I.; Huang, G. F.; Estrada, S.; Ausen, B.; Debnath, M. L.; Barletta, J.; Price, J. C.; Sandell, J.; Lopresti, B. J.; Wall, A.; Koivisto, P.; Antoni, G.; Mathis, C. A.; Langstrom, B.

Imaging brain amyloid in Alzheimer's disease with Pittsburgh Compound-B. *Ann. Neurol.* **2004**, *55*, 306−319.
(6) Villain, N.; Chetelat, G.; Grassiot, B.; Bourgeat, P.; Jones, G.; Ellis, K. A.; Ames, D.; Martins, R. N.; Eustache, F.; Salvado, O.; Masters, C. L.; Rowe, C. C.; Villemagne, V. L. Regional dynamics of amyloid-β deposition in healthy elderly, mild cognitive impairment and Alzheimer's disease: a voxelwise PiB-PET longitudinal study. *Brain* **2012**, *135*, 2126−2139.
(7) Driscoll, I.; Troncoso, J. C.; Rudow, G.; Sojkova, J.; Pletnikova, O.; Zhou, Y.; Kraut, M. A.; Ferrucci, L.; Mathis, C. A.; Klunk, W. E.; O'Brien, R. J.; Davatzikos, C.; Wong, D. F.; Resnick, S. M. Correspondence between in vivo ^{11}C-PiB-PET amyloid imaging and postmortem, region-matched assessment of plaques. *Acta Neuropathol.* **2012**, *124*, 823−831.
(8) Wong, D. F.; Rosenberg, P. B.; Zhou, Y.; Kumar, A.; Raymont, V.; Ravert, H. T.; Dannals, R. F.; Nandi, A.; Brasic, J. R.; Ye, W.; Hilton, J.; Lyketsos, C.; Kung, H. F.; Joshi, A. D.; Skovronsky, D. M.; Pontecorvo, M. J. In vivo imaging of amyloid deposition in Alzheimer disease using the radioligand ^{18}F-AV-45 (florbetapir F 18). *J. Nucl. Med.* **2010**, *51*, 913−920.
(9) Joshi, A. D.; Pontecorvo, M. J.; Clark, C. M.; Carpenter, A. P.; Jennings, D. L.; Sadowsky, C. H.; Adler, L. P.; Kovnat, K. D.; Seibyl, J. P.; Arora, A.; Saha, K.; Burns, J. D.; Lowrey, M. J.; Mintun, M. A.; Skovronsky, D. M. Performance characteristics of amyloid PET with florbetapir F 18 in patients with alzheimer's disease and cognitively normal subjects. *J. Nucl. Med.* **2012**, *53*, 378−384.
(10) Doraiswamy, P. M.; Sperling, R. A.; Coleman, R. E.; Johnson, K. A.; Reiman, E. M.; Davis, M. D.; Grundman, M.; Sabbagh, M. N.; Sadowsky, C. H.; Fleisher, A. S.; Carpenter, A.; Clark, C. M.; Joshi, A. D.; Mintun, M. A.; Skovronsky, D. M.; Pontecorvo, M. J. Amyloid-β assessed by florbetapir F 18 PET and 18-month cognitive decline: a multicenter study. *Neurology* **2012**, *79*, 1636−1644.
(11) Rowe, C. C.; Ackerman, U.; Browne, W.; Mulligan, R.; Pike, K. L.; O'Keefe, G.; Tochon-Danguy, H.; Chan, G.; Berlangieri, S. U.; Jones, G.; Dickinson-Rowe, K. L.; Kung, H. P.; Zhang, W.; Kung, M. P.; Skovronsky, D.; Dyrks, T.; Holl, G.; Krause, S.; Friebe, M.; Lehman, L.; Lindemann, S.; Dinkelborg, L. M.; Masters, C. L.; Villemagne, V. L. Imaging of amyloid β in Alzheimer's disease with ^{18}F-BAY94−9172, a novel PET tracer: proof of mechanism. *Lancet Neurol.* **2008**, *7*, 129−135.
(12) Barthel, H.; Luthardt, J.; Becker, G.; Patt, M.; Hammerstein, E.; Hartwig, K.; Eggers, B.; Sattler, B.; Schildan, A.; Hesse, S.; Meyer, P. M.; Wolf, H.; Zimmermann, T.; Reischl, J.; Rohde, B.; Gertz, H. J.; Reininger, C.; Sabri, O. Individualized quantification of brain β-amyloid burden: results of a proof of mechanism phase 0 florbetaben PET trial in patients with Alzheimer's disease and healthy controls. *Eur. J. Nucl. Med. Mol. Imaging* **2011**, *38*, 1702−1714.
(13) Barthel, H.; Gertz, H. J.; Dresel, S.; Peters, O.; Bartenstein, P.; Buerger, K.; Hiemeyer, F.; Wittemer-Rump, S. M.; Seibyl, J.; Reininger, C.; Sabri, O. Cerebral amyloid-β PET with florbetaben (^{18}F) in patients with Alzheimer's disease and healthy controls: a multicentre phase 2 diagnostic study. *Lancet Neurol.* **2011**, *10*, 424−435.
(14) Nelissen, N.; Van Laere, K.; Thurfjell, L.; Owenius, R.; Vandenbulcke, M.; Koole, M.; Bormans, G.; Brooks, D. J.; Vandenberghe, R. Phase 1 study of the Pittsburgh compound B derivative ^{18}F-flutemetamol in healthy volunteers and patients with probable Alzheimer disease. *J. Nucl. Med.* **2009**, *50*, 1251−1259.
(15) Vandenberghe, R.; Van Laere, K.; Ivanoiu, A.; Salmon, E.; Bastin, C.; Triau, E.; Hasselbalch, S.; Law, I.; Andersen, A.; Korner, A.; Minthon, L.; Garraux, G.; Nelissen, N.; Bormans, G.; Buckley, C.; Owenius, R.; Thurfjell, L.; Farrar, G.; Brooks, D. J. ^{18}F-flutemetamol amyloid imaging in Alzheimer disease and mild cognitive impairment: a phase 2 trial. *Ann. Neurol.* **2010**, *68*, 319−329.
(16) Cui, M.; Ono, M.; Kimura, H.; Liu, B.; Saji, H. Novel quinoxaline derivatives for in vivo imaging of β-amyloid plaques in the brain. *Bioorg. Med. Chem. Lett.* **2011**, *21*, 4193−4196.
(17) Yu, P.; Cui, M.; Wang, X.; Zhang, X.; Li, Z.; Yang, Y.; Jia, J.; Zhang, J.; Ono, M.; Saji, H.; Jia, H.; Liu, B. ^{18}F-labeled 2-phenylquinoxaline derivatives as potential positron emission tomography probes for in vivo imaging of β-amyloid plaques. *Eur. J. Med. Chem.* **2012**, *57*, 51−58.
(18) Zhang, W.; Kung, M. P.; Oya, S.; Hou, C.; Kung, H. F. ^{18}F-labeled styrylpyridines as PET agents for amyloid plaque imaging. *Nucl. Med. Biol.* **2007**, *34*, 89−97.
(19) Ono, M.; Watanabe, R.; Kawashima, H.; Kawai, T.; Watanabe, H.; Haratake, M.; Saji, H.; Nakayama, M. ^{18}F-labeled flavones for in vivo imaging of β-amyloid plaques in Alzheimer's brains. *Bioorg. Med. Chem.* **2009**, *17*, 2069−2076.
(20) Ono, M.; Watanabe, R.; Kawashima, H.; Cheng, Y.; Kimura, H.; Watanabe, H.; Haratake, M.; Saji, H.; Nakayama, M. Fluoro-pegylated chalcones as positron emission tomography probes for in vivo imaging of β-amyloid plaques in Alzheimer's disease. *J. Med. Chem.* **2009**, *52*, 6394−6401.
(21) Hsiao, K.; Chapman, P.; Nilsen, S.; Eckman, C.; Harigaya, Y.; Younkin, S.; Yang, F.; Cole, G. Correlative memory deficits, Aβ elevation, and amyloid plaques in transgenic mice. *Science* **1996**, *274*, 99−102.
(22) Kung, M. P.; Hou, C.; Zhuang, Z. P.; Zhang, B.; Skovronsky, D.; Trojanowski, J. Q.; Lee, V. M.; Kung, H. F. IMPY: an improved thioflavin-T derivative for in vivo labeling of β-amyloid plaques. *Brain Res.* **2002**, *956*, 202−210.
(23) Ono, M.; Watanabe, H.; Kimura, H.; Saji, H. BODIPY-based molecular probe for imaging of cerebral β-amyloid plaques. *ACS Chem. Neurosci.* **2012**, *3*, 319−324.
(24) Snellman, A.; Rokka, J.; Lopez-Picon, F. R.; Eskola, O.; Wilson, I.; Farrar, G.; Scheinin, M.; Solin, O.; Rinne, J. O.; Haaparanta-Solin, M. Pharmacokinetics of [^{18}F]flutemetamol in wild-type rodents and its binding to beta amyloid deposits in a mouse model of Alzheimer's disease. *Eur. J. Nucl. Med. Mol. Imaging* **2012**, *39*, 1784−1795.